

## SENSITIVITY IMPROVEMENTS IN UNCOOLED MICROBOLOMETER FPAS\*

August 1998

W. Radford, R. Wyles, J. Wyles, J. Varesi, M. Ray, D. Murphy, A. Kennedy, and A. Finch,  
Raytheon Infrared Center of Excellence  
Goleta, CA 93117

E. Moody, F. Cheung, R. Coda, and S. Baur  
Raytheon Systems Company  
El Segundo, CA 90245

### ABSTRACT

Raytheon Systems Company has developed a prototype infrared imaging rifle-sight using an uncooled, microbolometer FPA. The high-sensitivity FPA (SBRC-151) used in the Long-wavelength Staring Sensor (LWSS) was developed by Raytheon Infrared Center of Excellence (IR COE). The NETD (noise equivalent temperature difference) sensitivity of the camera has been measured at 14 mK with  $f/1$  optics and at 74 mK with an  $f/2.1$  aperture stop. Excellent imagery has been demonstrated with the  $f/2.1$  aperture. The  $320 \times 240$  FPA utilizes a high-yield CMOS readout integrated circuit (ROIC) that achieves high sensitivity, low output nonuniformity, and large scene dynamic range. The ROIC provides multi-level, on-chip nonuniformity correction and on-chip temperature compensation. The FPA has  $50 \mu\text{m} \times 50 \mu\text{m}$  pixels and operates at frame rates up to 60 Hz with a single output.

The LWSS was characterized by the US Army's NVESD in 1997 using an earlier version of the SBRC-151 FPA. The NVESD measurements validated the Raytheon NETD data. The NVESD evaluation also demonstrated outstanding MRT and spatial noise characteristics.

The  $\text{VO}_x$  microbolometer detectors are produced at the Raytheon IR COE facility in Santa Barbara, CA using an advanced dry-etch fabrication process. In addition to the LWSS project, the IR COE has initiated production of the microbolometer FPAs (AE-189) for commercial applications. Over 600 FPAs have been produced on this project, and data is presented for the first 250 FPAs that have been packaged and tested. The pixel operability of the production radiometer FPAs (AE-189) is typically greater than 99.9%.

### 1. INTRODUCTION

There is a critical need within the DOD for low-cost infrared sensors that provide good performance in compact, light-weight, low-power packages. Infrared focal plane arrays (FPAs) have been developed for a wide range of military applications including FLIRs, missile seekers,IRSTs, and strategic surveillance applications. Current second generation FPAs are typically hybrid structures comprised of a photovoltaic detector array and a silicon integrated circuit. InSb detector arrays are typically used for MWIR (3-5  $\mu\text{m}$ ) applications, and HgCdTe are typically used for LWIR (8-14  $\mu\text{m}$ ) applications. These FPAs offer near-BLIP sensitivities but must be operated at temperatures around 78K. These cryogenic operating temperatures necessitate the use of refrigerators and complex vacuum packaging. For these reasons cryogenic IRFPAs are costly and have power and reliability limitations.

\* Work partially supported by SBRC IR&D and DARPA IRFPA/FM Uncooled FPA program (Contract No. DAAB07-94-C-M001). DARPA Program Manager -- Ray Balcerak. NVESD Contract Monitor -- Jim Miller.

# REPORT DOCUMENTATION PAGE

Form Approved OMB No.  
0704-0188

Public reporting burden for this collection of information is estimated to average 1 hour per response, including the time for reviewing instructions, searching existing data sources, gathering and maintaining the data needed, and completing and reviewing this collection of information. Send comments regarding this burden estimate or any other aspect of this collection of information, including suggestions for reducing this burden to Department of Defense, Washington Headquarters Services, Directorate for Information Operations and Reports (0704-0188), 1215 Jefferson Davis Highway, Suite 1204, Arlington, VA 22202-4302. Respondents should be aware that notwithstanding any other provision of law, no person shall be subject to any penalty for failing to comply with a collection of information if it does not display a currently valid OMB control number. PLEASE DO NOT RETURN YOUR FORM TO THE ABOVE ADDRESS.

<b>1. REPORT DATE (DD-MM-YYYY)</b> 01-08-1998		<b>2. REPORT TYPE</b> Conference Proceedings		<b>3. DATES COVERED (FROM - TO)</b> xx-xx-1998 to xx-xx-1998	
<b>4. TITLE AND SUBTITLE</b> Sensitivity Improvements in Uncooled Microbolometer FPAS Unclassified			<b>5a. CONTRACT NUMBER</b>		
			<b>5b. GRANT NUMBER</b>		
			<b>5c. PROGRAM ELEMENT NUMBER</b>		
<b>6. AUTHOR(S)</b> Radford, W. ; Wyles, R. ; Wyles, J. ; Varesi, J. ; Ray, M. ;			<b>5d. PROJECT NUMBER</b>		
			<b>5e. TASK NUMBER</b>		
			<b>5f. WORK UNIT NUMBER</b>		
<b>7. PERFORMING ORGANIZATION NAME AND ADDRESS</b> Raytheon Infrared Center of Excellence Goleta, CA93117			<b>8. PERFORMING ORGANIZATION REPORT NUMBER</b>		
<b>9. SPONSORING/MONITORING AGENCY NAME AND ADDRESS</b> Director, CECOM RDEC Night Vision and Electronic Sensors Directorate 10221 Burbeck Road Ft. Belvoir, VA22060-5806			<b>10. SPONSOR/MONITOR'S ACRONYM(S)</b>		
			<b>11. SPONSOR/MONITOR'S REPORT NUMBER(S)</b>		
<b>12. DISTRIBUTION/AVAILABILITY STATEMENT</b> APUBLIC RELEASE					
<b>13. SUPPLEMENTARY NOTES</b> See Also ADM201041, 1998 IRIS Proceedings on CD-ROM.					
<b>14. ABSTRACT</b> Raytheon Systems Company has developed a prototype infrared imaging rifle-sight using an uncooled, microbolometer FPA. The high-sensitivity FPA (SBRC-151) used in the Longwavelength Staring Sensor (LWSS) was developed by Raytheon Infrared Center of Excellence (IR COE). The NETD (noise equivalent temperature difference) sensitivity of the camera has been measured at 14 mK with f/1 optics and at 74 mK with an f/2.1 aperture stop. Excellent imagery has been demonstrated with the f/2.1 aperture. The 320 x 240 FPA utilizes a high-yield CMOS readout integrated circuit (ROIC) that achieves high sensitivity, low output nonuniformity, and large scene dynamic range. The ROIC provides multi-level, on-chip nonuniformity correction and on-chip temperature compensation. The FPA has 50 mm x 50 mm pixels and operates at frame rates up to 60 Hz with a single output. The LWSS was characterized by the US Army's NVESD in 1997 using an earlier version of the SBRC-151 FPA. The NVESD measurements validated the Raytheon NETD data. The NVESD evaluation also demonstrated outstanding MRT and spatial noise characteristics. The VOX microbolometer detectors are produced at the Raytheon IR COE facility in Santa Barbara, CA using an advanced dry-etch fabrication process. In addition to the LWSS project, the IR COE has initiated production of the microbolometer FPAs (AE-189) for commercial applications. Over 600 FPAs have been produced on this project, and data is presented for the first 250 FPAs that have been packaged and tested. The pixel operability of the production radiometer FPAs (AE-189) is typically greater than 99.9%.					
<b>15. SUBJECT TERMS</b>					
<b>16. SECURITY CLASSIFICATION OF:</b>		<b>17. LIMITATION OF ABSTRACT</b>	<b>18. NUMBER OF PAGES</b>	<b>19. NAME OF RESPONSIBLE PERSON</b>	
a. REPORT Unclassified	b. ABSTRACT Unclassified	c. THIS PAGE Unclassified	Public Release	12	Fenster, Lynn lfenster@dtic.mil
				<b>19b. TELEPHONE NUMBER</b>	
				International Area Code Area Code Telephone Number 703767-9007 DSN 427-9007	
					Standard Form 298 (Rev. 8-98) Prescribed by ANSI Std Z39.18

The development of monolithic FPAs that operate at room temperatures will lead to significant improvements in the cost and reliability of IR FPA products. Specific applications include manportable sensors such as rifle-sights, missile launch units, and helmet mounted sights. Applications also include drivers aids for military vehicles. In addition the development of low-cost FPAs opens the possibility of using these devices for commercial applications such as automotive driver aids, industrial monitoring, and security surveillance systems.

## 2. BACKGROUND AND HISTORY

Room temperature IRFPAs have been in development for military applications since the late 1970s. Room temperature LWIR FPAs typically rely upon a thermal detection mode rather than the photovoltaic mode used for cryogenic systems. A key performance limiting characteristic for thermal detectors is the thermal isolation. The theory for the operation of thermal detectors has been discussed extensively.<sup>1,2</sup> Work on room temperature FPAs initially focused on hybrid FPAs based on bulk ferroelectric detectors<sup>3</sup>. These detectors have an inherent AC-coupled response but require a chopper for operation. The bulk detectors also have limitations on the pixel thermal isolation that can be achieved.

Higher sensitivity thermal detectors are being developed using micromachining fabrication techniques. Microbridge structures are being utilized in order to achieve thermal isolation values that are within a factor of ten of theoretical limits. Microbolometers readily lend themselves to the planar configurations that are necessary for fabrication on microbridge structures<sup>4,5</sup>. This technology has the potential for significant cost reduction compared to existing IR detector technologies. The monolithic array fabrication process is based on standard silicon IC processing. There is a tremendous potential for leveraging the large investments in developing silicon IC technology into low-cost uncooled IR detector sensors. Since cooling to cryogenic temperatures is not required, a major reduction in package complexity and cost will be achieved. Eliminating the need for cooling FPAs will also provide increased reliability, maintainability and operating life.

Raytheon Infrared Center of Excellence (IR COE) licensed the microbolometer FPA technology from Honeywell in 1993. The microbolometer pixel structure has been described in detail in other papers<sup>4,5</sup>. Two dimensional arrays of microbolometers are fabricated on silicon integrated circuit wafers using a surface micromachining technique. The microbolometer consists of a 0.5  $\mu\text{m}$  thick bridge of  $\text{Si}_3\text{N}_4$  suspended about 2  $\mu\text{m}$  above the underlying silicon substrate. The bridge is supported by two narrow legs of  $\text{Si}_3\text{N}_4$ . The  $\text{Si}_3\text{N}_4$  legs provide the thermal isolation between the microbolometer and the readout substrate.  $\text{Si}_3\text{N}_4$  is used because of its excellent thermal material properties (low thermal conductivity and low specific heat) and its excellent processing characteristics. Encapsulated in the center of the  $\text{Si}_3\text{N}_4$  bridge is a thin layer (500 $\text{\AA}$ ) of polycrystalline  $\text{VO}_x$ .  $\text{VO}_x$  is the temperature sensitive resistor material that makes the bolometer.  $\text{VO}_x$  is used as the bolometer material due to its combination of high temperature coefficient of resistance (TCR), acceptable electrical resistivity, and fabrication compatibility.

Raytheon Sensors and Electronics Systems (SES) has developed a manportable IR sensor that utilizes the SBRC-151 microbolometer FPA. This sensor is designed to take advantage of the cost, weight, and power advantages that are afforded by the microbolometer FPA technology. The RSC sensor has produced excellent imagery with an NETD of 14 mK (f/1.0 optics). The power consumption of the sensor is only 4.8 watts.

## 3. MICROBOLOMETER PIXEL FABRICATION

Raytheon IR COE has been actively fabricating microbolometer arrays since 1995. The microbolometer structure and its fabrication process has been improved significantly beyond that transferred in Honeywell license. This work has focused on improving the sensitivity of the detectors through better thermal isolation, higher fill-factor, and higher temperature coefficient of resistance. In addition these efforts have simultaneously emphasized simplifying the process to achieve better yields and faster cycle times.

Raytheon IR COE has implemented several improvements to the microbolometer fabrication process.<sup>6</sup> An advanced leg etch process has been implemented that reduced the leg width by a factor of two. This change increased the thermal isolation by a factor of two while allowing area for increased detector fill-factor. The key performance characteristics of Raytheon's microbolometer detectors are summarized in Table 1. Uniform pixel resistance is a key factor for achieving high-sensitivity microbolometer FPAs. Typical microbolometer readout circuits can accommodate peak-to-peak resistance nonuniformity of 10 percent and still achieve maximum sensitivity and pixel operability. The fabrication process has demonstrated a high yield of arrays that meet the resistance uniformity specification.

Table 1. Summary Of Design And Performance Characteristics Of Raytheon Microbolometers

Performance Parameter	Capability
Pixel Dimensions	50 $\mu\text{m}$ x 50 $\mu\text{m}$
Thermal Conductance	$< 5 \times 10^{-8}$ W/K
Thermal Time Constant	$< 20$ msec
Optical Fill-Factor	40%
Spectral Response	8 - 14 $\mu\text{m}$
Absorptivity	$> 80\%$
Resistance	50 Kohms Nominal
TCR	$> 2.2\%/C$
Resistance Nonuniformity	$< 10\%$ p-p

The most important change to the fabrication process is the use of a polyimide sacrificial layer material. The polyimide has been implemented in place of the baseline  $\text{SiO}_2$  sacrificial layer. It allows use of a dry sacrificial etch rather than the wet HF-based etch used in the baseline process. The elimination of the wet etch has dramatically simplified the microbolometer fabrication process. The dry etch process has the advantage of a near zero etch rate of the  $\text{Si}_3\text{N}_4$  used for the bridge. Similarly it has a zero etch rate for the oxides and metal layers used in the readout substrates. The wet etch used in the baseline process caused a measurable etching of the  $\text{Si}_3\text{N}_4$  and would strongly attack the underlying readout substrate layers. This necessitated additional processing steps to ensure that the readout was properly protected. The tendency for the wet etch to attack the underlying readout led to yield losses despite the incorporation of these additional steps. The benign nature of the dry etch results in yield improvements and allows simplification of the process to reduce cycle time. The tendency for the wet process to etch the  $\text{Si}_3\text{N}_4$  can also lead to both wafer-to-wafer variations and intrawafer spatial nonuniformity in the final thickness of the  $\text{Si}_3\text{N}_4$  bridges. This affect leads to variations in responsivity and response time.

The dry process facilitates several process and design changes to improve the microbolometer responsivity. It allows the thickness of the  $\text{Si}_3\text{N}_4$  layers to be reduced significantly without sacrificing device yield. The ability to fabricate the microbridges with thinner  $\text{Si}_3\text{N}_4$  layers will become increasingly important as smaller pixel sizes are developed. The deposition process of the  $\text{Si}_3\text{N}_4$  has been optimized for maximum production throughput and minimum thermal conductivity. The SBRC nitride deposition process can complete a 20-wafer lot in about one hour. The deposition process also produces films with very low stress. The thermal conductivity of the SBRC  $\text{Si}_3\text{N}_4$  is only about  $0.8 \text{ W}\cdot\text{m}^{-1}\cdot\text{K}^{-1}$ . This represents over a factor of two reduction of thermal conductivity compared with the baseline material. A scanning electron microphotograph of a microbolometer pixel fabricated with the dry sacrificial etch process and the optimized  $\text{Si}_3\text{N}_4$  is shown in Figure 1.

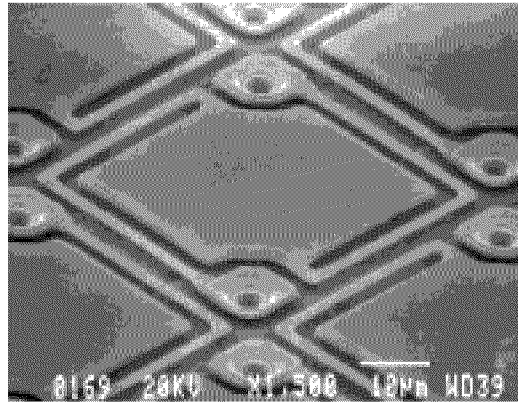


Figure 1. SEM Photograph Of Microbolometer Pixels Fabricated On CMOS Readout Circuit By Raytheon IR COE In Its Dedicated Silicon Detector Fabrication Facility.

#### 4. FPA ARCHITECTURE AND READOUT CIRCUIT DESIGN

Raytheon's microbolometer FPA provides very high sensitivity while maintaining a simple electrical interface to IR systems. The FPA has a 320 x 240 format with 50  $\mu\text{m}$  x 50  $\mu\text{m}$  pixels. The FPA responds to radiation in the LWIR (8 to 14  $\mu\text{m}$ ) spectral window. The performance characteristics of the SBRC-151 FPA are summarized in Table 2 and a photograph of the SBRC-151 is shown in Figure 2.

This FPA is based on a CMOS readout integrated circuit (ROIC). The ROIC uses on-chip clock and bias generation to provide a simple electrical interface requiring only three clocks and five bias levels. The ROIC architecture is an evolution of SBRC's first generation BiCMOS readout that was described previously.<sup>10,11</sup> The SBRC-151 ROIC operates in an electronically scanned format and pulse-biases each pixel. The key features and interface characteristics of this readout are summarized in Table 3. The ROIC provides a large gain to the detector signal. This ensures that sensor performance is limited by the FPA noise and responsivity. The SBRC-151 readout circuit performs on-chip offset correction to minimize spatial nonuniformity in the FPA output. The on-chip correction allows the use of a high detector bias (>4 volts) and on-chip gain without saturation of the output range. The readout utilizes a differential architecture throughout the signal chain in order to minimize sensitivity to bias fluctuation and external noise sources. These features give the SBRC-151 FPA very high responsivity and good extraneous noise immunity. The ROIC also incorporates an on-chip temperature compensation capability in order to minimize temperature stabilization requirements.

Table 2. Summary Of Performance Characteristics Of SBRC-151 Uncooled FPA.

Performance Parameter	Capability (f/1.0 and 300K Scene)
Array Configuration	320 x 240
Pixel Size	50 $\mu\text{m}$ x 50 $\mu\text{m}$
Overall Chip Dimensions	18.3 mm x 18.4 mm
Spectral Response	8 - 14 $\mu\text{m}$
Signal Responsivity	> $2.5 \times 10^7$ V/W or 50 mV/K <sub>scene</sub>
NETD @ f/1	< 20 mK
Offset Nonuniformity	< 150 mV p-p
Output Noise	1.0 mV RMS
Dynamic Range @ f/1	> 40 K
Pixel Operability	> 98%
Crosstalk (nearest neighbor)	< 1%
Nominal Operating Temperature	(Combined optical and electrical) 25° C

Table 3. Summary Of Interface Characteristics Of SBRC-151 ROIC.

Interface Parameter	Capability
Number of Clocks	3
Number of Bias Levels	5
On-chip Offset Correction	8-bits per pixel
Temperature Compensation	Incorporated in Input Circuit and Differential Architecture
Output Voltage Swing	2.0 V
Dynamic Range Control	Adjustable Input Circuit Gain and Output Gain
Operating Mode Control	32 bit Serial Programmable
Output Gain	Selectable (2x or 3.5x)
Maximum Frame Rate	60 Hz
Outputs	1 -- RS 170 Compatible

The various operational and test modes of the chip are controlled through a 32-bit serial programmable interface. The ROIC was specifically designed to accommodate a wide range of detector impedances without degradation of sensitivity. The ROIC will operate with pixel impedances ranging from 10 Kohms to 200 Kohms with little degradation in performance. This tolerance to a wide range of pixel resistance allows the SBRC-151 to take advantage of increases in TCR that can be achieved with higher bolometer resistance values. The SBRC-151 has a wide range of programmable on-chip gain values. These features allow optimization of performance for a wide range of operating conditions as well as detector resistance values. These settings can also be used for optimization of dynamic range versus sensitivity for different applications. Several lots of SBRC-151 ROICs have been fabricated, and the yield of die with zero defective columns and rows is consistently greater than 30%. The ROIC yield increases to nearly 80% if four defective columns are allowed.

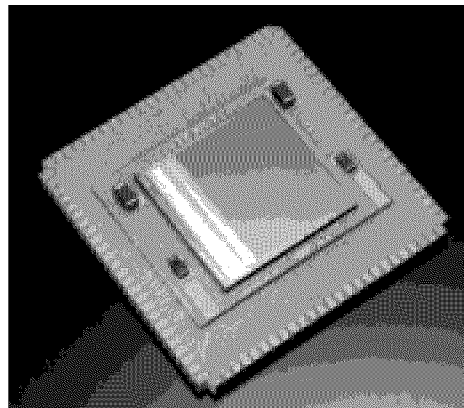


Figure 2. Photograph Of SBRC-151 Uncooled Microbolometer FPA

Several SBRC-151 microbolometer FPAs have been assembled into vacuum packages in order to conduct performance testing and imaging demonstrations. The SBRC-151 FPAs can be incorporated into either the ICC Type VI vacuum package (Figure 3) or into SBRC-designed vacuum packages. Both packages utilize an all-metal construction and are suitable for both military and commercial applications. The packages incorporate a low-cost single-stage thermo-electric cooler for temperature stabilization. An AR-coated Ge window provides high transmission in the 8 to 14  $\mu\text{m}$  spectral region. The packages are designed for a vacuum life in excess of ten years.



Figure 3. Photograph Of ICC Type VI Vacuum Package.

### 5. LWSS SENSOR AND ELECTRONICS

The Long-wavelength Staring Sensor (LWSS) is a prototype military infrared camera for manportable applications. The camera achieves low-power consumption in order to maximize battery life. The camera utilizes a sealed, all-metal housing that encloses the detective assembly, electronics boards and miniaturized CRT display. The camera utilizes a 50 mm focal length  $f/0.7$  Ge lens assembly with a broadband AR coating. The transmission of the optics is greater than 95%. The key features and performance characteristics of the LWSS sensor are summarized in Table 4. The camera has a power consumption of 4.8 watts. The weight of the prototype camera is 6.5 pounds. Straight-forward modifications have been identified that will reduce the weight of the productized camera to less than 4 pounds. The LWSS camera provides memory for both the coarse on-chip correction terms as well as the gain and offset nonuniformity correction terms. The offset correction terms are performed as a field calibration. A photograph of the LWSS camera is shown in Figure 4.

Table 4. Summary Of Sensor Electronics Functions And Features.

Sensor Function
8-Bit Coarse Correction (On FPA)
12- Bit A/D
Two-point Correction
RS-170 and Digital Outputs
Symbology and Reticule Displays
2:1 Digital Zoom
Video Polarity Reversal
Automatic and manual Gain/Level Control
Defective Pixel Substitution
9 mm x 12 mm RS-170 CRT
$\pm 2\text{mK}$ FPA Temperature Stabilization
4.8 Watts Power Consumption

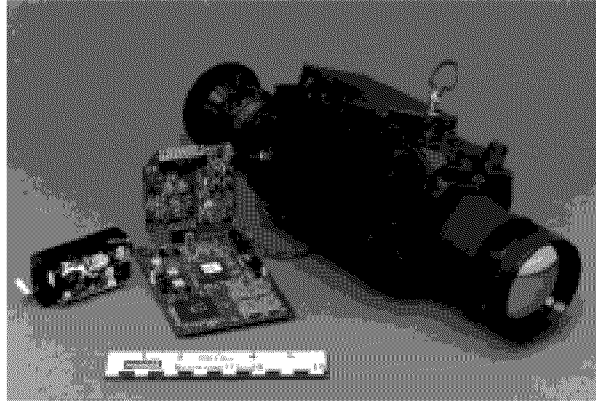


Figure 4. Photograph Of LWSS Camera.

The LWSS electronics consists of a power supply board, detector interface board and a digital signal processing board. These boards are shown in Figure 4 along with the LWSS camera body. User interface controls on the camera can adjust the output level, contrast, polarity, reticule displays, and digital zoom. User control knobs also allow calibration of the offset correction terms. The LWSS operates with 60 Hz field rates from the FPA and can perform a two-field averaging prior to display. The LWSS also incorporates a 2:1 digital zoom capability.

The power supply is designed to be compatible with standard batteries and has an 83% conversion efficiency. The temperature stabilization control circuit for the single-stage thermo-electric cooler is also incorporated on the power supply board. The temperature control circuit has been designed to achieve a FPA temperature stabilization of  $\pm 2$  mK. The detector interface board provides the low-noise bias supplies for the FPA and provides level shifting of the detector video output.

The digital signal processing board performs a wide range of functions including user interface control, generation of FPA timing clocks, control nonuniformity correction, and other signal processing operations. The DSP is controlled by a microprocessor and uses an FPGA for timing functions and image processing. The DSP provides the clock signals to the FPA along with the 8-bit data words for on-chip coarse correction. The video signal from the FPA is sent to a 12 bit analog/digital converter. The DSP then performs gain and offset nonuniformity correction. The other functions performed by the DSP include automatic gain control, field averaging, 2:1 digital zoom, as well as reticule and symbology generation. The DSP provides an RS-170 output to the miniature CRT display. In addition it has auxiliary outputs for both RS-170 and digital formats.

## 6. LWSS PERFORMANCE CHARACTERISTICS

The LWSS sensor has been used for imaging demonstrations and radiometric testing of the SBRC-151 FPAs. Standard test conditions include a 298K operating temperature and illumination from a blackbody through the camera optics. The sensitivity data for a high performance FPA using an f/1.0 aperture is presented in Figure 5. The average NETD at f/1.0 is 14 mK. The pixel operability of this FPA is about 98%. The average NETD for the sensor with an f/2.1 aperture is 74 mK (Figure 6). The FPAs achieve high responsivity with an average of about 70 mV/K at f/1.0. The FPA exhibits a well-behaved gaussian noise distribution. The average noise level of 1 mV is dominated by the FPA contributions. The FPAs have also been used to obtain infrared imagery. An examples of this imagery obtained from the LWSS camera operating with an f/2.1 aperture is shown in Figure 7. Figure 8 presents data on the responsivity linearity of the SBRC-151 FPA. The maximum deviation of the responsivity from a linear fit is about 1%.



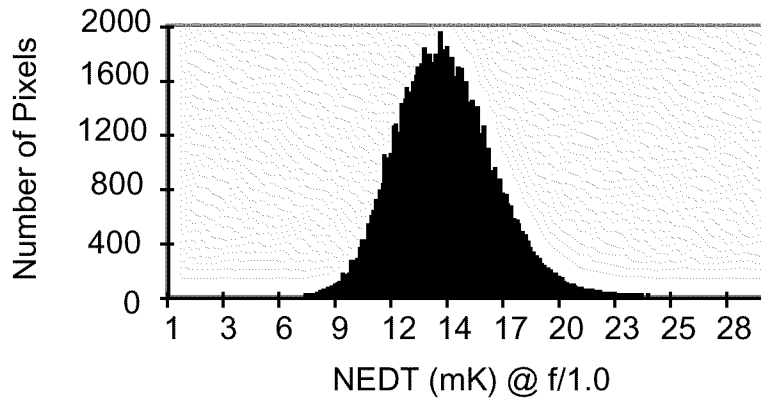


Figure 5. Raytheon LWSS Camera With SBRC-151 FPA Demonstrates Average NETD Of 14 mK With f/1 Optics.

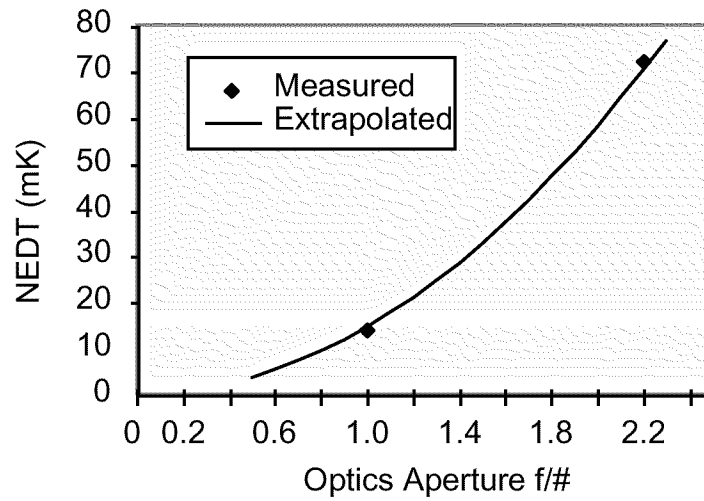


Figure 6. LWSS Camera has an average NETD Of 14 mK with f/1.0 Optics and 74 mK with f/2.1 Optics.

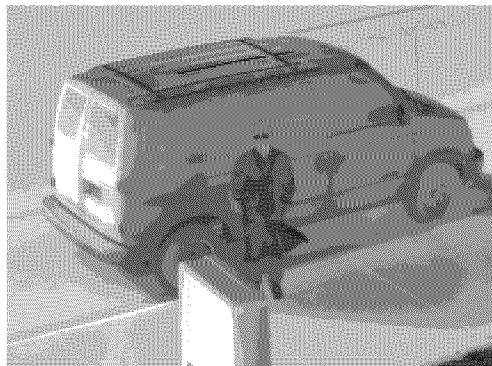


Figure 7. Single-Frame Image Obtained From LWSS Camera with f/2.1 Optics.

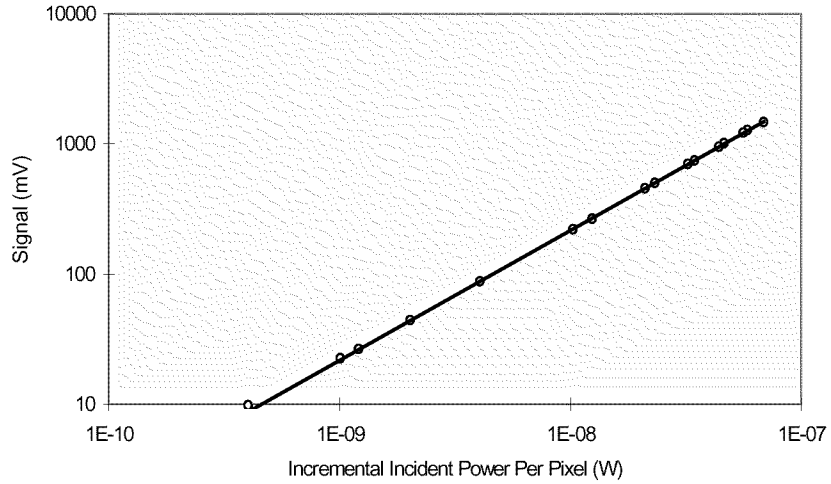


Figure 8. SBRC-151 Microbolometer FPAs Exhibit Excellent Uniformity Over a Wide Flux Range. Maximum Deviation from a Linear Fit is Approximately 1%.

The Raytheon LWSS camera was delivered to the US Army's Night Vision and Electronics Sensors Directorate (NVESD) during the summer of 1997. The performance of the LWSS camera was independently evaluated by test personnel at NVESD<sup>12</sup>. NVESD tests included NETD, MRT, and 3-D noise measurements. These data are summarized in Figure 9 and Table 5. At that time the LWSS camera was equipped with an earlier version of the SBRC-151 FPA. The camera was measured at Raytheon to have an NETD of 27mK at f/0.7 and 48 mK at f/1.0. The NVESD generally agreed well with the Raytheon measurements and confirmed the very high sensitivity achieved with the camera. The NVESD data also indicated that the spatial noise of the sensor was generally less than 50% of the temporal noise values. The 3-D noise values were measured approximately 2 hours after the last camera calibration.

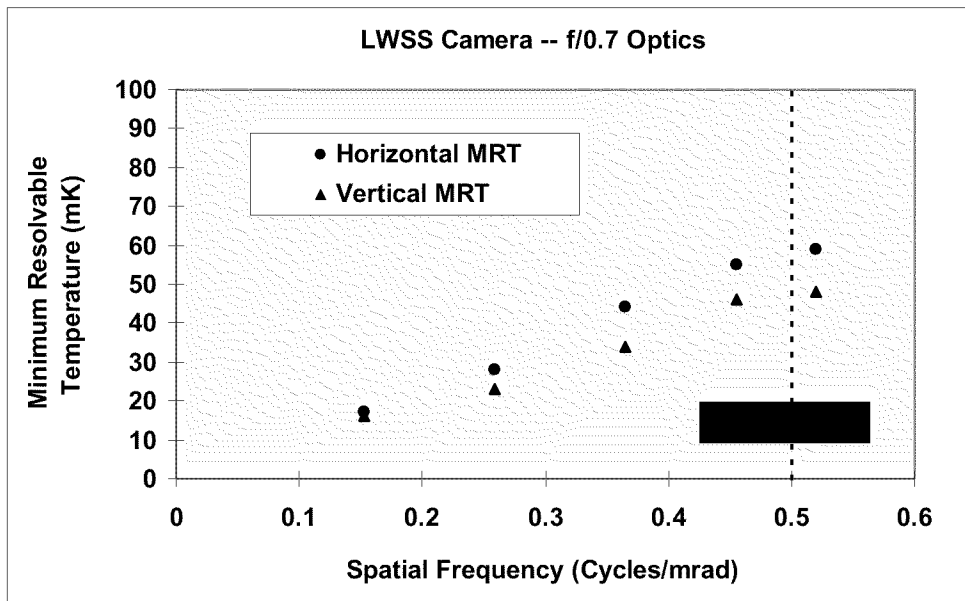


Figure 9. MRT Measurements Performed At NVESD in 1997 Demonstrate Excellent Sensitivity For LWSS Camera<sup>12</sup>.

Table 5. Summary Of NVESD Performance Measurements for LWSS Sensor with early version of SBRC-151 FPA.

Performance Parameter	f/0.7 Optics	f/1.0 Optics
NETD	24 mK	42 mK
3-D Noise Terms		
$t_{vh}$ (temporal random)	22.3 mK	37.7 mK
$t_v$ (temporal vertical)	12.8 mK	23.2 mK
$t_h$ (temporal horizontal)	3.1 mK	5.1 mK
$t$ (frame)	8.6 mK	16.8 mK
$vh$ (spatial random)	10.0 mK	19.0 mK
$v$ (spatial vertical)	3.6 mK	6.6 mK
$h$ (spatial horizontal)	6.0 mK	11.5 mK
Total 3-D Noise	28.7 mK	50.2 mK
Minimum Resolvable Temperature		
Horizontal MRT @ 0.520 cycles/mrad	59 mK	93 mK
Vertical MRT @ 0.520 cycles/mrad	48 mK	109 mK
Horizontal MRT @ 0.153 cycles/mrad	16 mK	31 mK
Vertical MRT @ 0.153 cycles/mrad	16 mK	36 mK

## 7. COMMERCIAL FPA PRODUCTION STATUS AND PERFORMANCE CHARACTERISTICS

Raytheon IR COE has also started low-rate production of a separate line microbolometer FPAs for commercial applications. These arrays are being fabricated primarily for the Raytheon ExplorIR commercial radiometer cameras<sup>7,8</sup>. The microbolometer arrays are fabricated on the Amber AE-189 readout wafers using a baseline fabrication process. These arrays have demonstrated outstanding performance with good yields. The microbolometer fabrication yields are typically between 50% and 60%. Figures 10 - 12 present producibility data achieved for the first 242 FPAs that have been packaged and tested. These FPAs were selected from several microbolometer fabrication lots<sup>9</sup>. Figure 10 presents a histogram of the array-average NETD values. The median f/0.74 NETD value for the first 242 FPAs is 44.5 mK. Figure 11 presents data on the pixel operability achieved on the same set of packaged FPAs. The median pixel operability of the FPAs is 99.88%. Figure 12 presents similar data on the responsivity nonuniformity. The median nonuniformity (std. dev./mean) for the AE-189 FPAs is 3.3%.

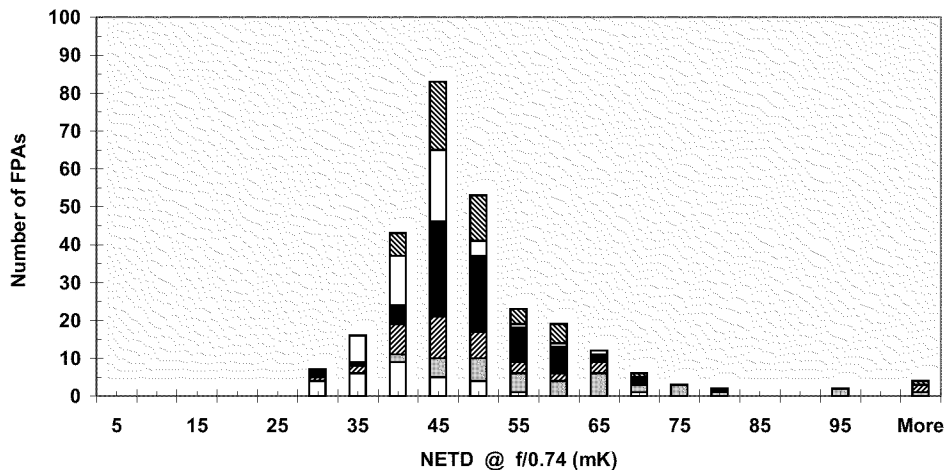


Figure 10. Array-Average NETD (f/0.74) of AE-189 Commercial Microbolometer FPAs Fabricated in IRCOE Facility. Median NETD of First 242 Packaged FPAs = 44.5 mK.

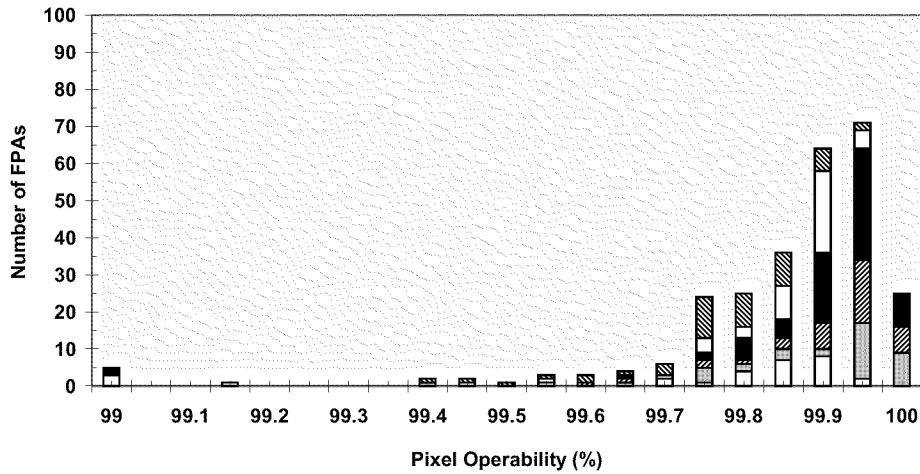


Figure 11. Pixel Operability of AE-189 FPAs Fabricated in IRCOE Facility. Median Pixel Operability (excluding defective columns) of First 242 Packaged FPAs = 99.88%.

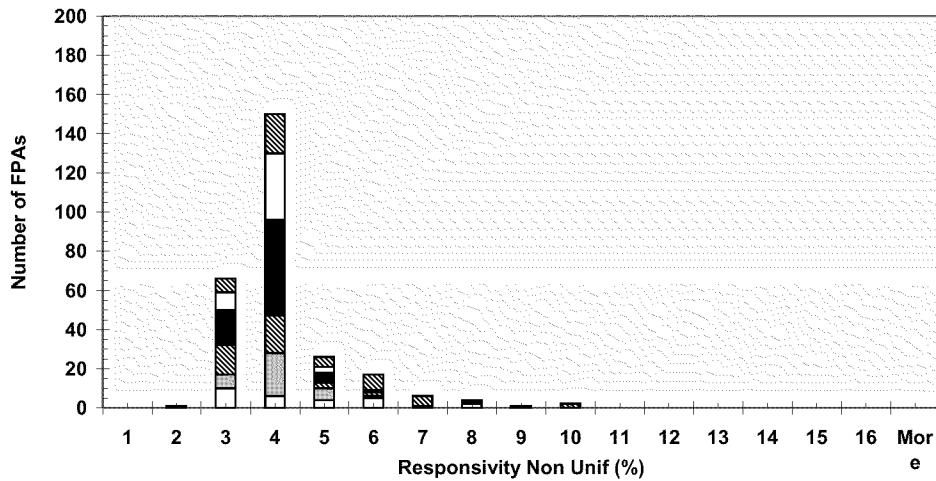


Figure 12. Uncorrected Responsivity Nonuniformity (Std Dev/Mean) of AE-189 FPAs Fabricated in IRCOE Facility. Median Nonuniformity of First 242 Packaged FPAs = 3.29%.

## 8. SUMMARY

Raytheon IR COE and Sensor and Electronics Systems has developed a prototype manportable imaging system based on uncooled microbolometer FPAs. The LWSS camera has demonstrated low-power and is suitable for manportable military applications. The LWSS camera has demonstrated high quality imagery with sensitivity levels of 14 mK with  $f/1.0$  optics and 74 mK with an  $f/2.1$  aperture. NETD and MRT measurements have been independently performed at NVESD. The 320 x 240 microbolometer FPAs were fabricated at SBRC on an advanced CMOS readout circuit using an advanced microbolometer fabrication process. The novel readout circuit performs a high degree of on-chip processing to maximize sensitivity. Raytheon IR COE has also initiated production of microbolometer FPAs for commercial applications.

## 9. REFERENCES

- <sup>1</sup> R.B. Emmons, S.R. Hawkins, and K.F. Cuff, "Infrared Detectors: An Overview," *Optical Engineering*, Vol. 14(1), pp 21-30, 1975.
- <sup>2</sup> E.H. Putley, "Thermal Detectors," in Topics in Applied Physics, Vol. 19: Optical and Infrared Detectors, pp. 71-100, R.J. Keyes, editor, Springer-Verlag, New York, 1980.
- <sup>3</sup> D. Dudley and K.D. Peterson, "High-Density Uncooled Focal Plane Array Development," Proceedings of IRIS Detector Specialty Group, pp. 197-206, Boulder, CO. August, 1991.
- <sup>4</sup> R.A. Wood, B.E. Cole, C.J. Han, and R.E. Higashi, "High-performance Uncooled Microbolometer Focal Planes," Proceedings of IRIS Detector Specialty Group, Bedford, MA. August, 1993.
- <sup>5</sup> R.A. Wood, C.J. Han, and P.W. Kruse, "Integrated Uncooled Infrared Detector Imaging Arrays," IEEE Solid State Sensor and Actuator Workshop, pp.132-135, Hilton Head Island, SC. June 1992.
- <sup>6</sup> W. Radford, D. Murphy, M. Ray, J. Kojiro, K. Platt, A. Kennedy, J. Spagnolia, A. Finch, R. Coda, G. Lung, E. Moody, D. Gleichman, and S. Baur, "Advanced Microbolometer Pixels for Uncooled IR FPAs," Proceedings of IRIS Detector Specialty Group, Boulder, CO. July 1996.
- <sup>7</sup> B. Meyer, A. Stout, A. Gin, P. Taylor, E. Woodbury, J. Deffner, and F. Ennerson, "Hand Held Thermal Viewer Based on Amber 320 x 240 Microbolometer FPA," Proceedings of IRIS Passive Sensors Specialty Group, Monterey, CA. March 1996.
- <sup>8</sup> R. Cannatta, G. Kincaid, R. Hanson, C. Madden, A. Gin, and R. Higashi, "320 x 240 Uncooled Microbolometer Focal Plane Array," Proceedings of IRIS Passive Sensors Specialty Group, Monterey, CA. March 1996.
- <sup>9</sup> Data on AE-189 pixel operability and responsivity uniformity provided by T. Hoelter, R. Cannatta, and L. Padgett of Raytheon-Amber.
- <sup>10</sup> W. Radford, D. Murphy, M. Ray, S. Propst, A. Kennedy, J. Kojiro, J. Woolaway, K. Soch, R. Coda, G. Lung, E. Moody, D. Gleichman, and S. Baur, "320 x 240 Silicon Microbolometer Uncooled IRFPAs with On-chip Offset Correction," Proceedings of IRIS Passive Sensors Specialty Group, Monterey, CA. March 1996.
- <sup>11</sup> D. Murphy, W. Radford, M. Ray, S. Propst, A. Kennedy, J. Kojiro, J. Woolaway, K. Soch, R. Coda, G. Lung, E. Moody, D. Gleichman, and S. Baur, "320 x 240 Silicon Microbolometer Uncooled IRFPAs with On-chip Offset Correction," Proceedings of SPIE, Vol. 2746, pp. 82-92, April 1996.
- <sup>12</sup> NVESD test data on LWSS sensor acquired by S. Prucnic and B. Cronk.